

Collective migration of leukocytes

Adriano Barra

Dipartimento di Matematica & Fisica, Università del Salento



USA and Italy: Biomechanists Outlining New Directions

Workshop

September 24-27, 2023

Naples, Italy

OUTLINE OF THE TALK

- 1) The Maximum Entropy Principle à la Jaynes & a minimal historical overview
- 2) The migration of leukocytes toward cancer in LabOnChips as a stochastic process
- 3) Inferring the interactions: delayed max-S (path integral formulation)
- 4) Application One: dendritic migrations as uncorrelated drifter random walks
- 5) Application Two: evaluation of chemotherapy efficacy in pancreatic cancer
- 6) Outlooks and conclusions

The starting point: inverse problems in the statistical mechanics of neural networks

Weak pairwise correlations imply strongly correlated network states in a neural population

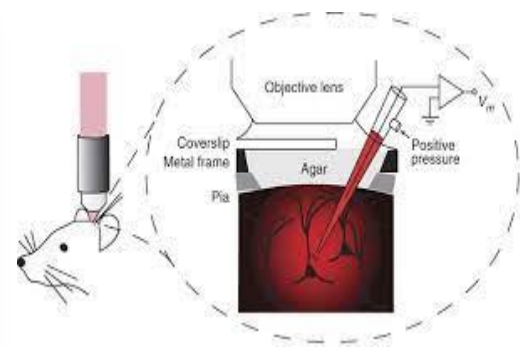
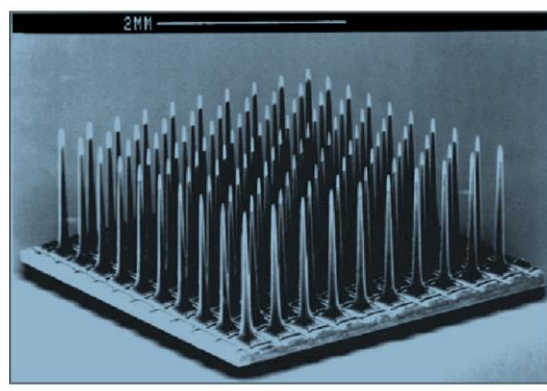
Know $(J, h) \rightarrow$ generate neural configuration $\{\sigma\} \rightarrow$ **Direct Problem.**
 Know neural configuration $\{\sigma\} \rightarrow$ infer $(J, h) \rightarrow$ **Inverse Problem.**

Elad Schneidman^{1,2,3}, Michael J. Berry II², Ronen Segev² & William Bialek^{1,3}

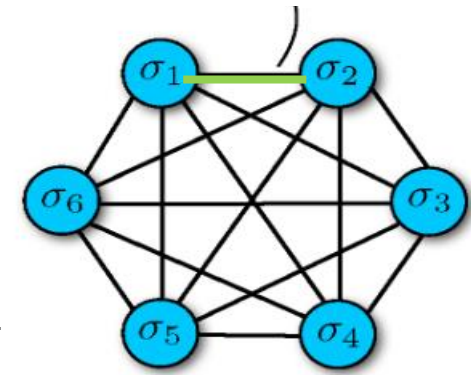
$$H(\sigma, J, h) = - \sum_{i < j}^{N, N} J_{ij} \sigma_i \sigma_j - \sum_i^N h_i \sigma_i.$$

Protocol: Patch-clamp and multi-electrode array electrophysiological analysis in acute mouse brain slices

$$P_\infty(\sigma) = \frac{e^{-\beta H(\sigma, J, h)}}{Z(\beta, J, h)}.$$



$\sigma_i = \pm 1$



Hopfield Network



Interaction ruling animal collective behavior depends on topological rather than metric distance: Evidence from a field study

M. Ballerini^{*†}, N. Cabibbo^{‡§}, R. Candelier^{†¶}, A. Cavagna^{*||**}, E. Cisbani[†], I. Giardina^{*||}, V. Lecomte^{††††}, A. Orlandi^{*}, G. Parisi^{*‡§***}, A. Procaccini^{*‡}, and M. Viale^{‡§§}, and V. Zdravkovic^{*}

^{*}Centre for Statistical Mechanics and Complexity (SMC), Consiglio Nazionale delle Ricerche-Istituto Nazionale per la Fisica della Materia, [†]Dipartimento di Fisica, and [§]Sezione Istituto Nazionale di Fisica Nucleare, Università di Roma "La Sapienza," Piazzale Aldo Moro 2, 00185 Roma, Italy; ^{††}Istituto Superiore di Sanità, viale Regina Elena 299, 00161 Roma, Italy; ^{||}Istituto dei Sistemi Complessi (ISC), Consiglio Nazionale delle Ricerche, via dei Taurini 19, 00185 Roma, Italy; and ^{†††}Laboratoire Matière et Systèmes Complexes, (Centre National de la Recherche Scientifique Unite Mixte de Recherche 7057), Université Paris VII, 10 rue Alice Domon et Léonie Duquet, 75205 Paris Cedex 13, France

Contributed by G. Parisi, December 4, 2007 (sent for review September 25, 2007)



Statistical mechanics for natural flocks of birds

William Bialek^a, Andrea Cavagna^{b,c}, Irene Giardina^{b,c,1}, Thierry Mora^d, Edmondo Silvestri^{b,c}, Massimiliano Viale^{b,c}, and Aleksandra M. Walczak^e

PRL 113, 117204 (2014)

PHYSICAL REVIEW LETTERS

week ending
12 SEPTEMBER 2014

Inverse Spin Glass and Related Maximum Entropy Problems

Michele Castellana^{1,*} and William Bialek^{1,2}

¹Joseph Henry Laboratories of Physics and Lewis-Sigler Institute for Integrative Genomics, Princeton University, Princeton, New Jersey 08544, USA

Phenomenal flocking

ARTIFICIAL SPIN ICE

Topologically induced vertex frustration

QUANTUM INFORMATION

Approximation for fast state estimation

TOPOLOGICAL SUPERCONDUCTORS

Underdoping does it

The maximum entropy distribution consistent with the directional correlations C_{ij} is

$$P(\{\vec{s}_i\}) = \frac{1}{Z(\{J_{ij}\})} \exp\left[\frac{1}{2} \sum_{i=1}^N \sum_{j=1}^N J_{ij} \vec{s}_i \cdot \vec{s}_j\right], \quad [1]$$

where $Z(\{J_{ij}\})$ is the appropriate normalization factor, or partition function; the derivation follows ref. 10, as explained in the *SI Appendix*. Notice that there is one parameter J_{ij} corresponding to each measured element C_{ij} of the correlation matrix. To finish the construction of the model, we have to adjust the values of the J_{ij} to match the experimentally observed C_{ij} ,

$$\langle \vec{s}_i \cdot \vec{s}_j \rangle_P = \langle \vec{s}_i \cdot \vec{s}_j \rangle_{\text{exp}}, \quad [2]$$

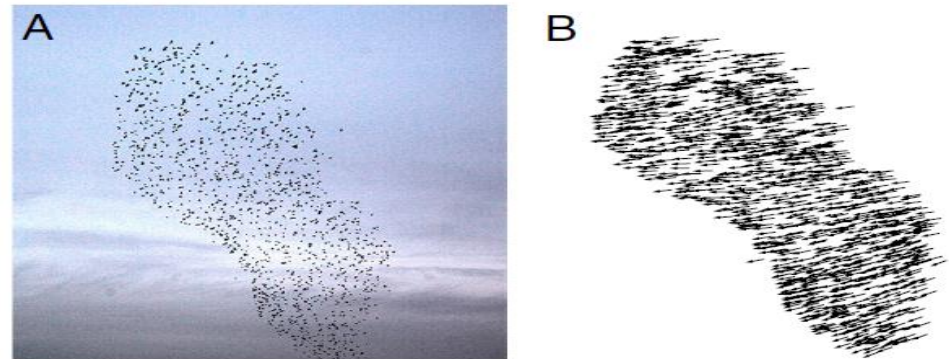


Fig. 1. The raw data. (A) One snapshot from flocking event 28–10, $N = 1,246$ birds (see *SI Appendix, Table S1*). (B) Instantaneous vector velocities of all the individuals in this snapshot, normalized as $\vec{s}_i = \vec{v}_i / |\vec{v}_i|$.

spins i and j , where $J > 0$ means that these elements tend to align. For many physical systems, once we know the Hamiltonian there is a plausible dynamics that allows the system to relax toward equilibrium, which is the Langevin dynamics

$$\frac{d\vec{s}_i}{dt} = -\frac{\partial H}{\partial \vec{s}_i} + \vec{\eta}_i(t) = \sum_{j=1}^N J_{ij} \vec{s}_j + \vec{\eta}_i(t), \quad [3]$$

The maximum entropy principle

History: Max-(log)likelihood estimation 1920. Max-entropy estimation 1950.

The problem is to find the *best* probability distribution $P(x)$ of a variable $x \in \Omega$ about which only certain information has been collected, as for instance the empirical moments, e.g the mean $\bar{x} = (1/N) \sum_i^N x_i$, the empirical variance σ_{exp}^2 , etc.

We want the theoretical moments to match the values of the empirical counterpart, i.e.

$$\bar{x} = \frac{1}{N} \sum_i^N x_i \quad \leftarrow \quad \bar{x} = \langle x \rangle, \quad \rightarrow \quad \langle x \rangle := \int_{\Omega} x P(x) dx.$$

etc.

We write the Shannon entropy $S[P]$ of the (unknown) $P(x)$ as

$$H[P] = \sum_{x \in \Omega} P(x) \ln P(x) \quad (0.1)$$

and we constraint its extremization via Lagrange multipliers that force the matching among the collected empirical information and the expected one so to obtain the *less structured* $P(x)$ in agreement with experimental measurements.



Example 1. Let us first assume that nothing is known about X . Thus the only constraint on p is that it should be normalized. So one has to solve

$$p^* = \operatorname{argmax}_p \{H[p]\} \quad \text{subject to} \quad \sum_{x \in \Omega} p(x) = 1$$

This is done by introducing a Lagrange parameter, conveniently written as $k\lambda_0$, and solving an unconstrained maximization problem for

$$H_{\lambda_0}[p] = H[p] + k\lambda_0 \left(\sum_{x \in \Omega} p(x) - 1 \right)$$

$$H[P] = \sum_{x \in \Omega} P(x) \ln P(x)$$

Thus p^* is found by solving

$$\frac{\partial H_{\lambda_0}[p]}{\partial p(x)} = -k \ln p(x) - k + k\lambda_0 = 0, \quad \forall x \in \Omega$$

$$\frac{\partial H_{\lambda_0}[p]}{\partial \lambda_0} = k \left(\sum_{x \in \Omega} p(x) - 1 \right) = 0$$

Principle of sufficient reason

The first set of equations require

$$p(x) = \exp(\lambda_0 - 1) = \text{const.}$$

The second imposes the normalization constraint, and entails

$$p^*(x) = \exp(\lambda_0 - 1) = |A|^{-1}$$

Gottfried Wilhelm Leibniz



Portrait by Christoph Bernhard Francke, 1695

Example 2. Here we take the average of X to be known, and given by μ_1 . This constitutes a second constraint, over and above the one of normalization. In this case one has to solve

$$p^* = \underset{p}{\operatorname{argmax}}\{H[p]\} \quad \text{subject to} \quad \sum_{x \in \Omega} p(x) = 1 \quad \text{and} \quad \sum_{x \in \Omega} p(x)x = \mu_1 = \frac{1}{N} \sum_i^N x_i$$

With the help of Lagrange multipliers as above, this translates into an unconstrained maximization problem for

$$H_{\lambda_0, \lambda_1}[p] = H[p] + k\lambda_0 \left(\sum_{x \in \Omega} p(x) - 1 \right) + k\lambda_1 \left(\sum_{x \in \Omega} p(x)x - \mu_1 \right)$$

The maximizing distribution is found by solving

$$\frac{\partial H_{\lambda_0, \lambda_1}[p]}{\partial p(x)} = -k \ln p(x) - k + k\lambda_0 + k\lambda_1 x = 0, \quad \forall x \in A$$

$$\frac{\partial H_{\lambda_0, \lambda_1}[p]}{\partial \lambda_0} = k \left(\sum_{x \in \Omega} p(x) - 1 \right) = 0$$

$$\frac{\partial H_{\lambda_0, \lambda_1}[p]}{\partial \lambda_1} = k \left(\sum_{x \in \Omega} p(x)x - \mu_1 \right) = 0$$

The solution can be written as

$$p^*(x) = \exp(\lambda_0 - 1 + \lambda_1 x) = \frac{1}{Z} \exp(\lambda_1 x)$$



Example 3. Of particular relevance to the continuous case is another example, where both the first moment $\mu_1 = \langle x \rangle$ and the second moment $\mu_2 = \langle x^2 \rangle$ of a real random variable X , with $A = \mathbb{R}$, are known. The best estimate for the probability density p in this case is found by determining the unconstrained maximum of

$$\begin{aligned} \tilde{H}_{\lambda_0, \lambda_1, \lambda_2}[p] = & \tilde{H}[p] + k\lambda_0 \left(\int dx p(x) - 1 \right) + k\lambda_1 \left(\int dx p(x)x - \mu_1 \right) \\ & + k\lambda_2 \left(\int dx p(x)x^2 - \mu_2 \right) \end{aligned}$$

in which integrals extend over \mathbb{R} . Following the established procedures, one finds a solution of the form

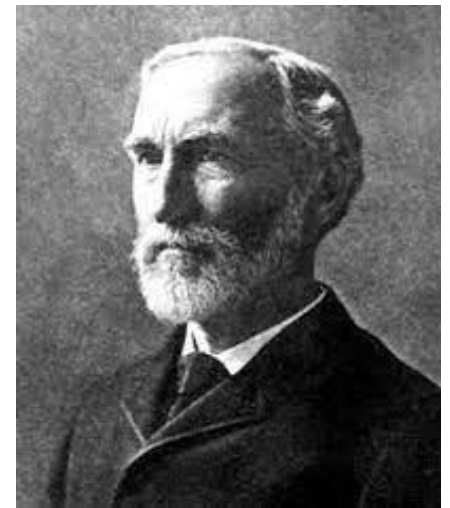
$$p^*(x) = \frac{1}{Z} e^{\lambda_1 x + \lambda_2 x^2} \quad (13.33)$$

For this solution to make sense, that is, be properly normalizable, we must obviously have $\lambda_2 < 0$. A minute of reflection then shows that the solution can be rewritten in the form

$$p^*(x) = \frac{1}{Z} e^{-(x - \hat{\lambda}_1)^2 / 2\hat{\lambda}_2}$$

with $\hat{\lambda}_2 = -\frac{1}{2}\lambda_2$ and $\lambda_1 = \hat{\lambda}_1 / \hat{\lambda}_2$, and where Z is an appropriately redefined normalization constant. The reader will immediately realize that this is nothing but a Gaussian probability density function, and read off that

$$\hat{\lambda}_1 = \mu_1, \quad \hat{\lambda}_2 = \sigma^2 = \mu_2 - \mu_1^2, \quad \text{and} \quad Z = \sqrt{2\pi\sigma^2}$$



Spend a few words on
«Statistical Reductionism»



FROM NOW ON THIS IS MY RESEARCH!

OPEN

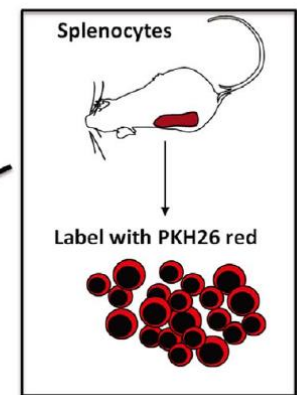
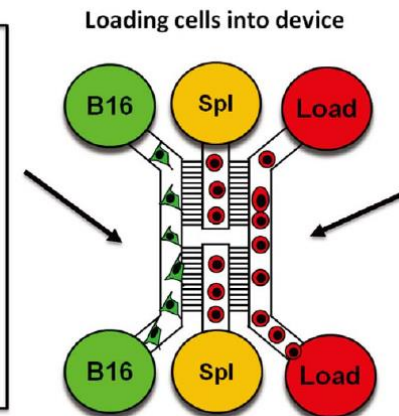
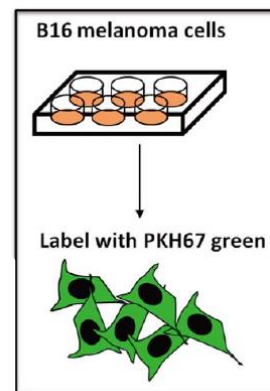
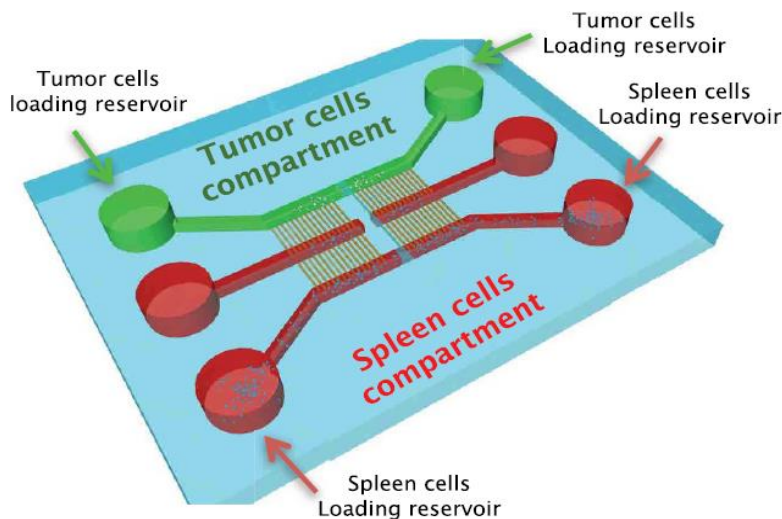
Cancer-driven dynamics of immune cells in a microfluidic environment

SUBJECT AREAS:

COMPUTATIONAL BIOPHYSICS

CANCER MICROENVIRONMENT

Elena Agliari¹, Elena Biselli¹, Adele De Ninno², Giovanna Schiavoni³, Lucia Gabriele³, Anna Gerardino⁴, Fabrizio Mattei³, Adriano Barra¹ & Luca Businaro⁴



Towards the development of human immune-system-on-a-chip platforms

Alessandro Polini^{1,2}, Loretta L. del Mercato², Adriano Barra^{1,3,4}, Yu Shrike Zhang⁵, Franco Calabi² and Giuseppe Gigli^{1,2}

Statistical tools to assess the migratory capabilities of leukocytes

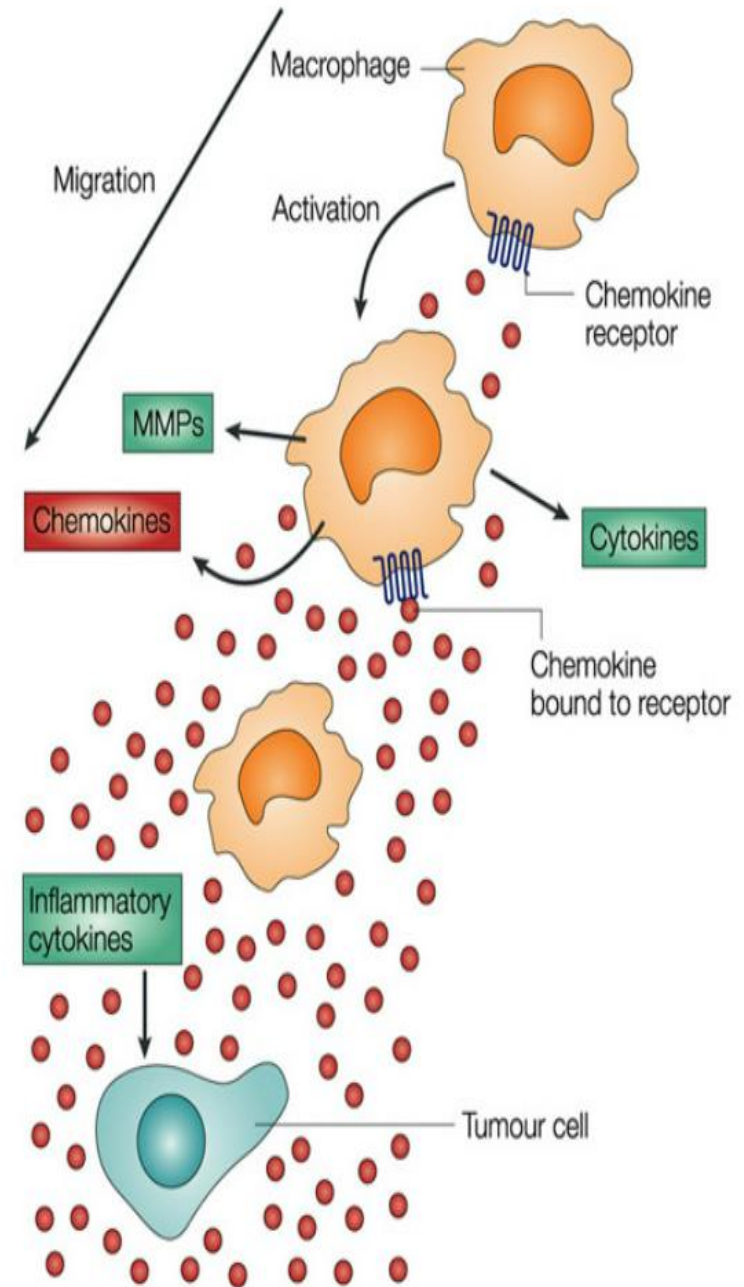
Introduction about players: searchers and targets

Motion of Leucocytes (in the presence of Pathogens)



At the site of the infection resident macrophages secrete cytokines

Chemotaxis mediated by Cytokines

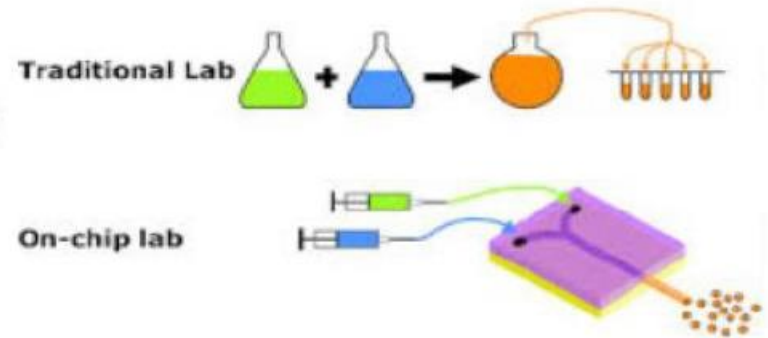


Methods

Lab-On-Chip experiment

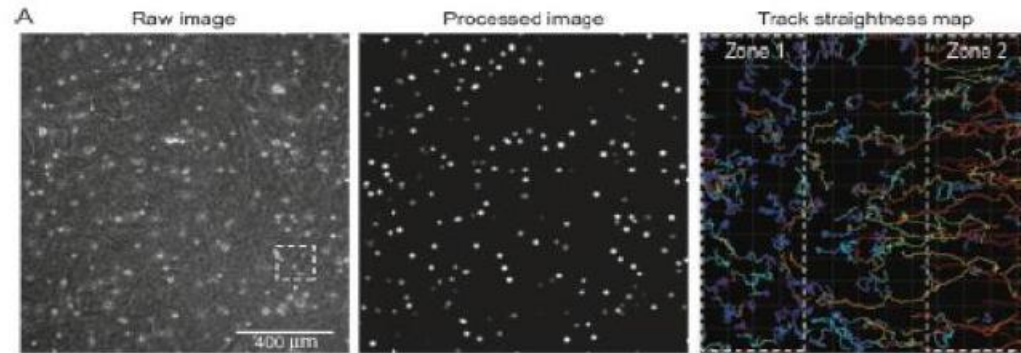
Reconstruction of cellular micro-environments exploiting microfluidic platforms and cellular co-cultures

- more natural than in-vitro exp.
- more controllable and cheaper than in-vivo exp.



Tracks of leukocytes

- #1
- $T_1 \ X_1 \ Y_1$
- $T_2 \ X_2 \ Y_2$
- ...
- $T_M \ X_M \ Y_M$
- #2
-

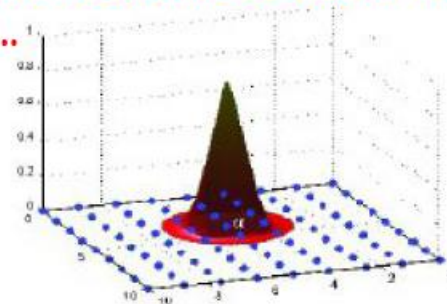


COMPUTAZIONALMENTE RICOSTRUIRE LE TRAIETTORIE E' AI ORA

Istituto Superiore di Sanità (Roma) **ma è stato the hell prima...**
Institut Curie - Department of Cell Biology (Paris)

Data Analysis

Modeling
Statistical inference



4 /28

Dal Time Lapse ricostruiamo lo spazio delle fasi e quindi, di nuovo, "physical tools behind"

The i -th track is looked at as a series of discrete steps
of length $\Delta r(i,t)$
and direction $\Theta(i,t)$,
for $i=1,\dots,N$ and $t=1,\dots,T_i$

Step lengths

$$V_x(i,t) \equiv \Delta X(i,t) = X(i,t+1) - X(i,t)$$

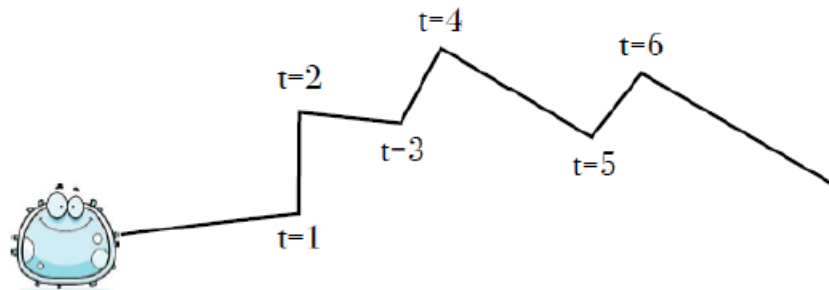
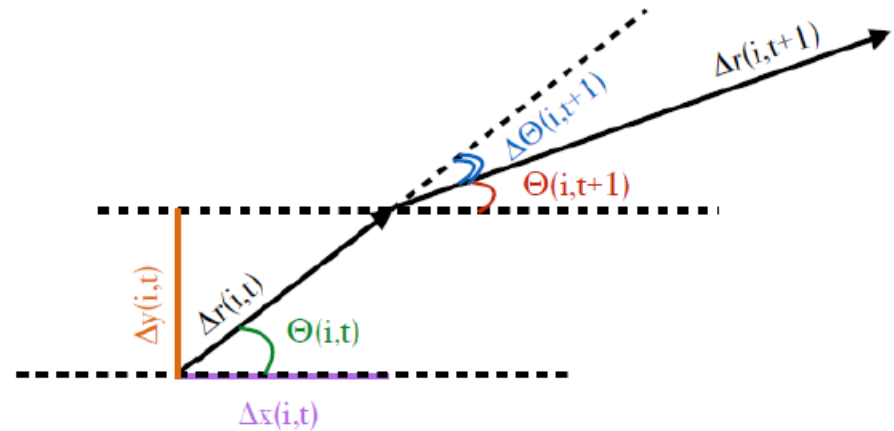
$$V_y(i,t) \equiv \Delta Y(i,t) = Y(i,t+1) - Y(i,t)$$

$$V(i,t) \equiv \Delta r(i,t) = \text{sqrt}[\Delta X^2(i,t) + \Delta Y^2(i,t)]$$

Direction

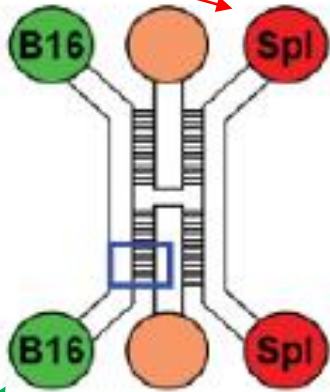
$$\Theta(i,t) = \text{atan}(\Delta Y(i,t) / \Delta X(i,t))$$

$$\Delta \Theta(i,t) = \Theta(i,t+1) - \Theta(i,t)$$



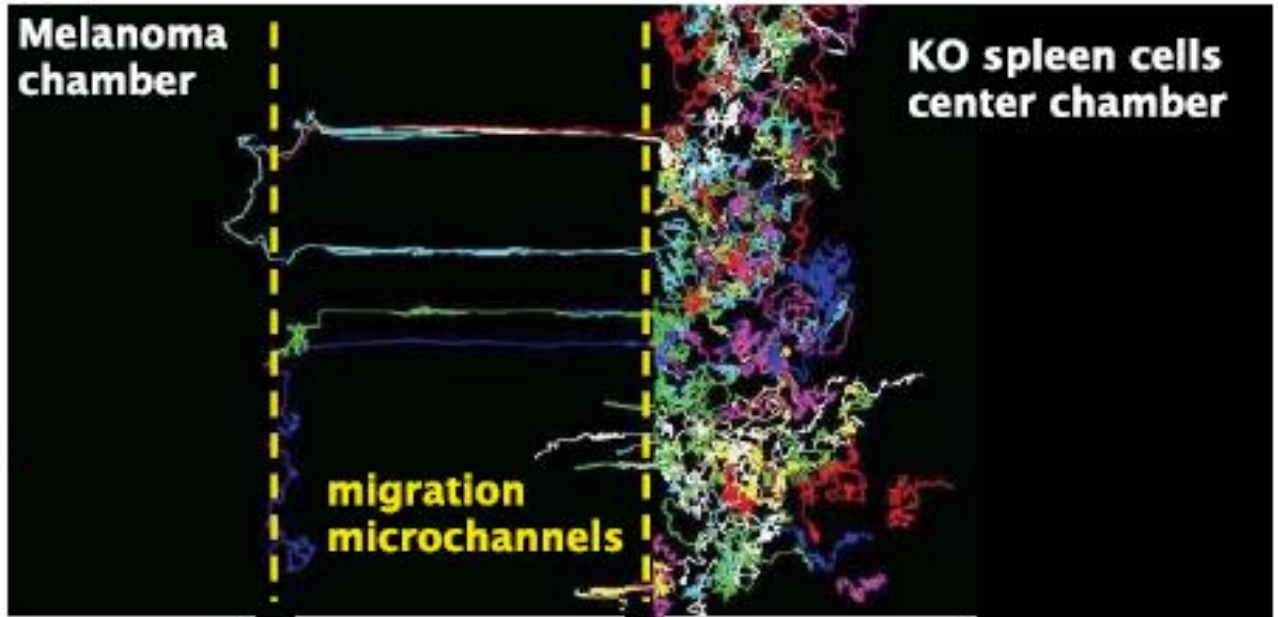
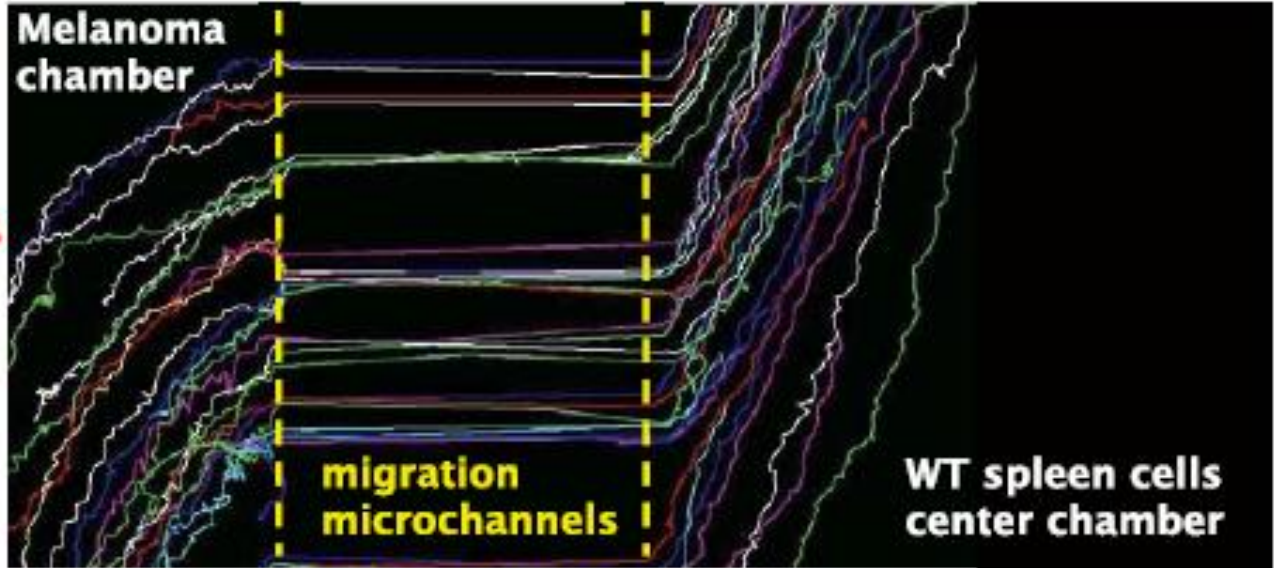
WT trajectories

Good guys reservoir



Bad guys reservoir

KO trajectories



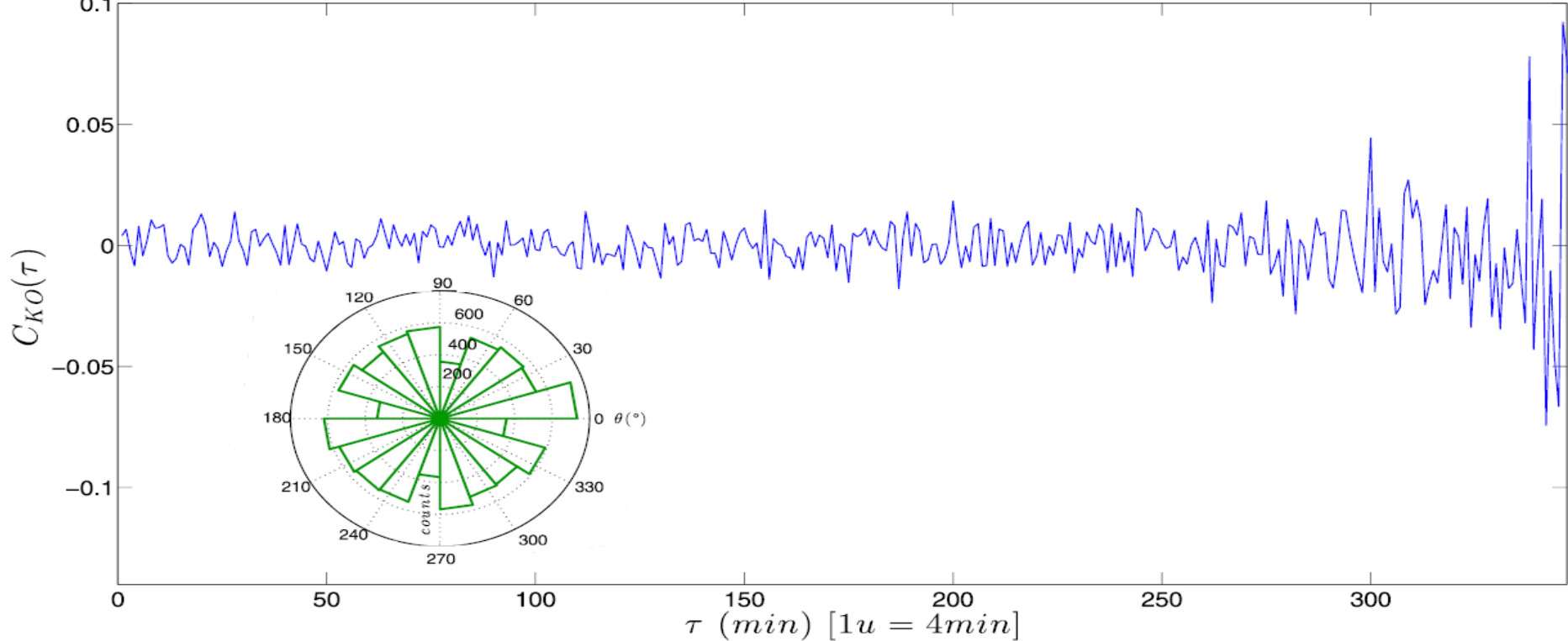


Figure 7 | Inset: polar histogram of the turning angle. The distribution has zero mean, hence, no angular correlation is observed. Main plot: angular correlation function $C_{KO}(\tau)$ of the turning angle θ . This correlation function shows more statistical noise at large τ .

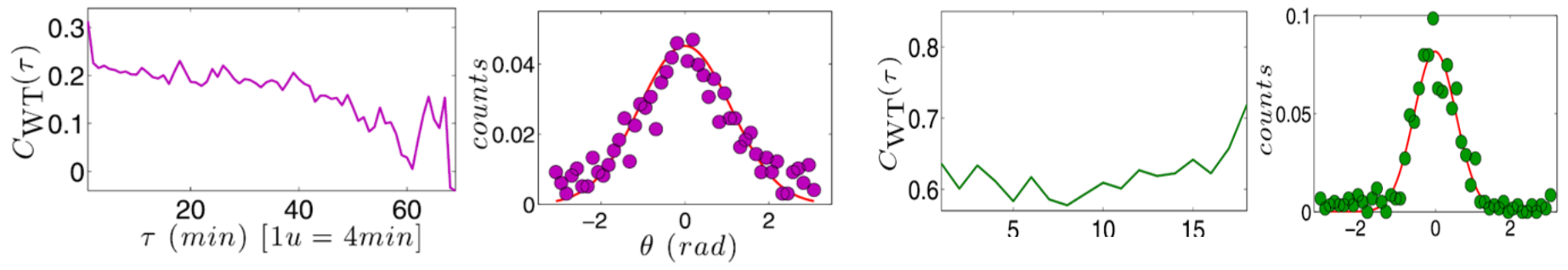


Figure 13 | Left panels: angular correlation function $C_{WT}(\tau)$ of the turning angle θ of WT-PRE splenocytes (upper panel) and of WT-POST splenocytes (lower panel). Right panels: histograms of the turning angle θ for WT-PRE (upper panel) and WT-POST (lower panel) splenocytes.

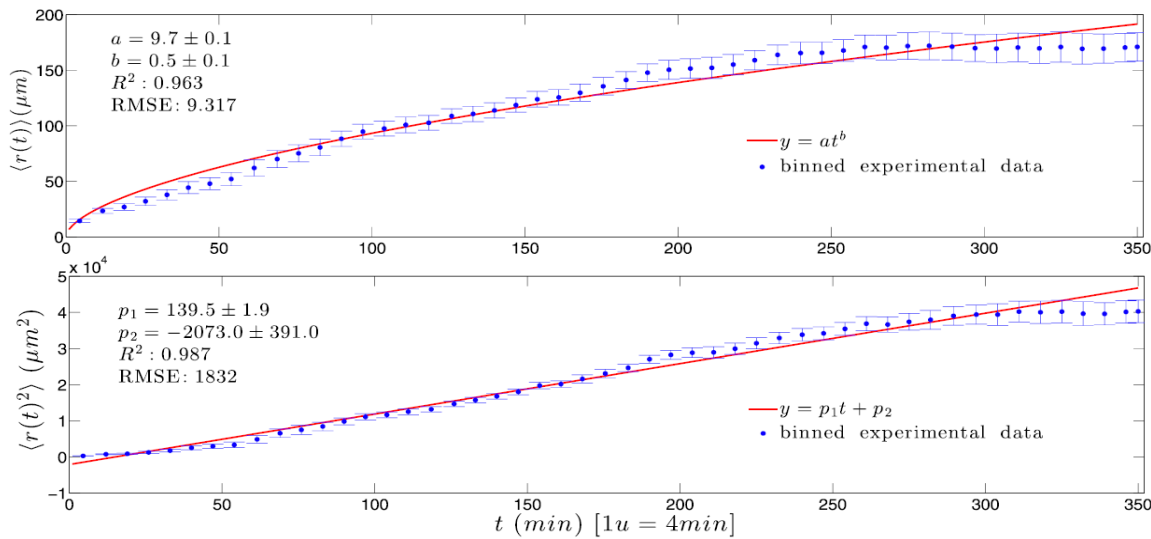
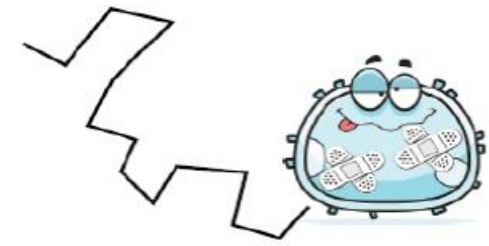


Figure 9 | Mean displacement $\langle r(t) \rangle$ (upper panel) and mean squared displacement $\langle r^2(t) \rangle$ (lower panel) for KO splenocytes. Experimental (binned) data (•) with standard errors are compared with best fits (solid line) whose coefficients are properly shown.



KO leukocytes perform standard diffusion.

OK (WT) leukocytes perform ballistic motion: they perceive the chemoattractant gradient.

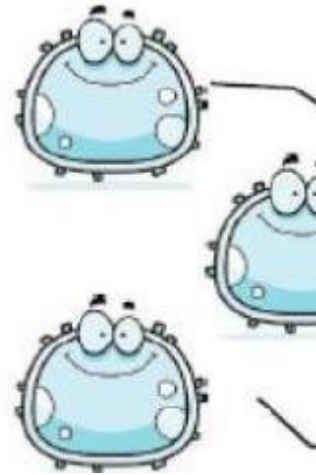
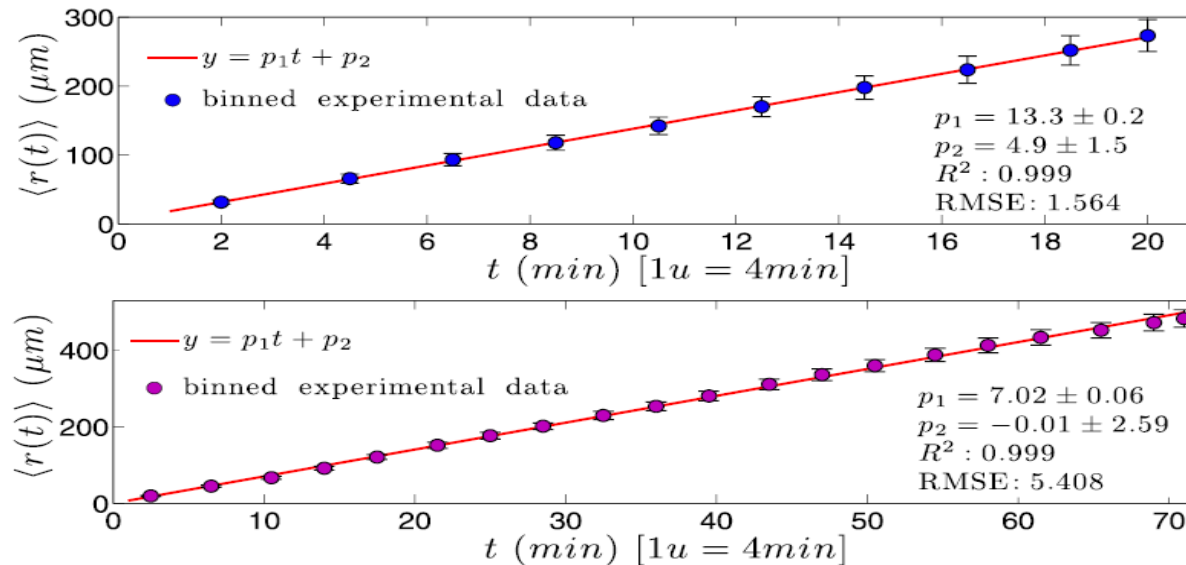
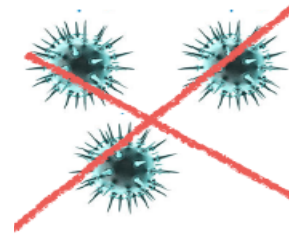
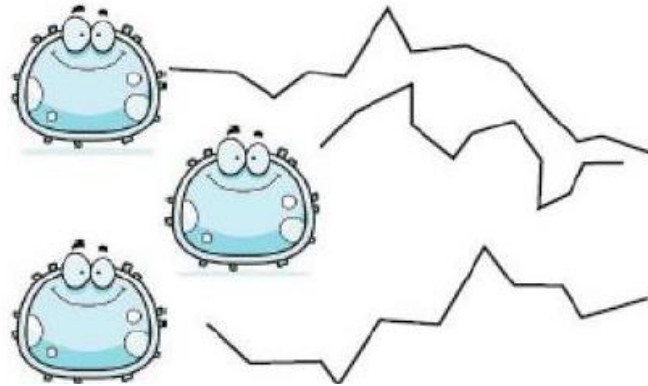


Figure 16 | $\langle r(t) \rangle$ versus t for WT-PRE splenocytes (upper panel) and for WT-POST splenocytes (lower panel). As expected, the mean displacement grows linearly with time. Binned data (•) with standard errors are compared with best fit (solid line), whose coefficients are also reported.

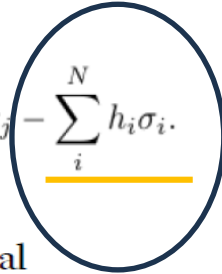
These leukocytes are «dendritic cells» (conclusions hold only for them)

Leukocytes in the absence of targets behave as “drunkard”, no matter their density
 No bias, no (auto)correlations among step lengths and directions



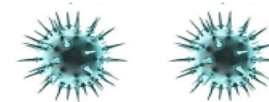
$$H(\sigma, J, h) = - \sum_{i < j}^{N, N} J_{ij} \sigma_i \sigma_j - \sum_i^N h_i \sigma_i$$

OK



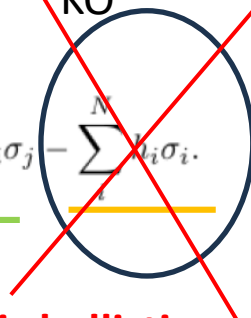
An analogous behavior is recovered for impaired leukocytes

Leukocytes are endowed by receptors, codified by particular genes, which feel gradients of chemical messengers (stemming from pathogens). If the gene is silenced, leukocytes are not aware of danger.



$$H(\sigma, J, h) = - \sum_{i < j}^{N, N} J_{ij} \sigma_i \sigma_j - \sum_i^N h_i \sigma_i$$

KO

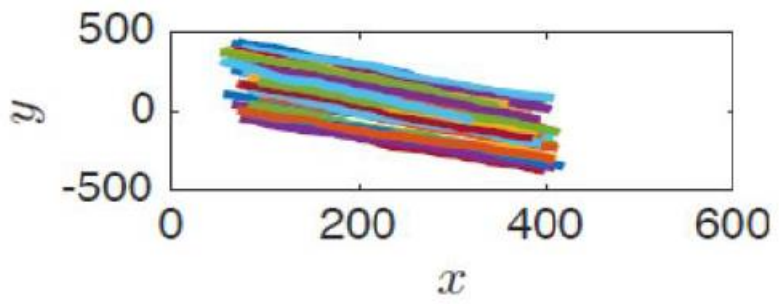
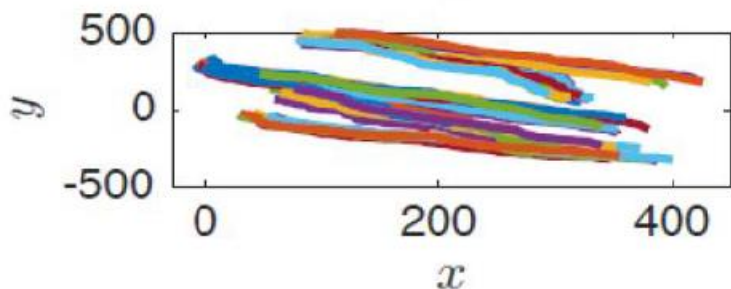
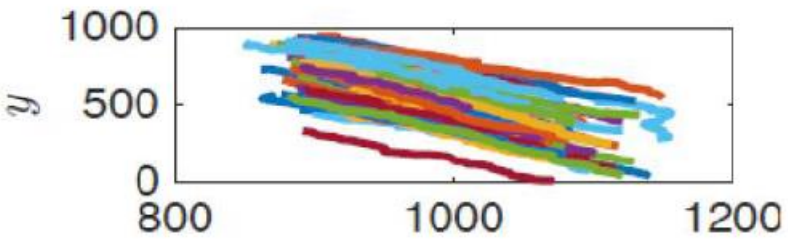


At contrary, if the white cells are healthy and the antigen is present, their motion is ballistic pointing straight to the target (i.e. the antigen).

A pivotal question concerns now «coordination» (or its lacking) during migration to antigen. Here the Maximum Entropy comes into help.

Often difficult to determine whether some tracks are aligned because of a field or because of a field & imitative interaction

Goal: develop a statistical methods able to answer easily (and possibly automatically) to this question.



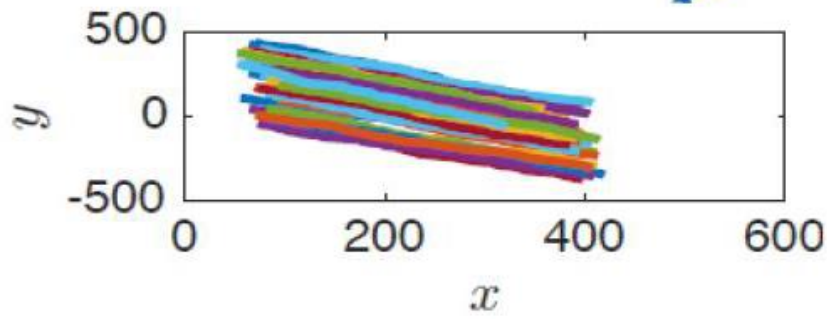
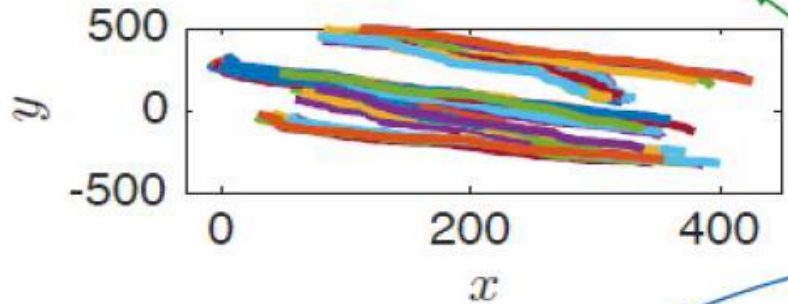
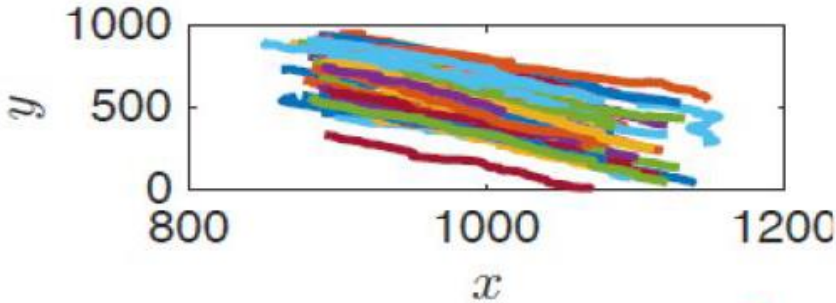
Comparable $\langle \vec{V}(i)\vec{V}(j) \rangle_{\text{exp}} - \langle \vec{V}(i) \rangle_{\text{exp}} \langle \vec{V}(j) \rangle_{\text{exp}}$ $\langle \vec{V}(i)\vec{V}(j) \rangle_{\text{exp}}$

- Cases:
- Coupling —
 - Field&Coupling — & —
 - Field —

$$H(\sigma, J, h) = - \sum_{i < j}^{N, N} J_{ij} \sigma_i \sigma_j - \sum_i^N h_i \sigma_i.$$

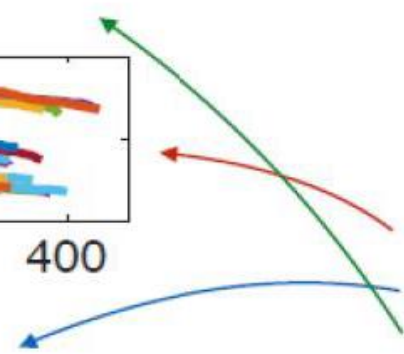
Often difficult to determine whether some tracks are aligned because of a field or because of a field & imitative interaction

Goal: develop a statistical methods able to answer easily (and possibly automatically) to this question.



Comparable $\langle \vec{V}(i)\vec{V}(j) \rangle_{\text{exp}} - \langle \vec{V}(i) \rangle_{\text{exp}} \langle \vec{V}(j) \rangle_{\text{exp}}$ $\langle \vec{V}(i)\vec{V}(j) \rangle_{\text{exp}}$

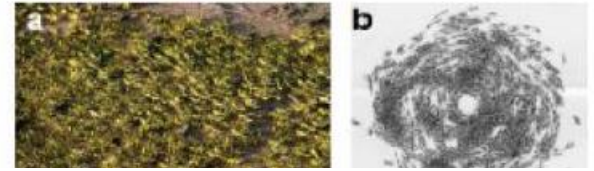
- Cases:
- Coupling
 - Field&Coupling
 - Field



Torniamo a noi: ma questi leucociti come migrano, indipendentemente o come dice Max Weber? 😊

The Maximum Entropy Approach

Collective motion



SCIENCE ADVANCES | RESEARCH ARTICLE

SYSTEMS BIOLOGY

A statistical inference approach to reconstruct intercellular interactions in cell migration experiments

Elena Agliari¹, Pablo J. Sáez², Adriano Barra³, Matthieu Piel²,
Pablo Vargas², Michele Castellana^{4,5*}

Migration of cells can be characterized by two prototypical types of motion: individual and collective migration. We propose a statistical inference approach designed to detect the presence of cell-cell interactions that give rise to collective behaviors in cell motility experiments. This inference method has been first successfully tested on synthetic motional data and then applied to two experiments. In the first experiment, cells migrate in a wound-healing model: When applied to this experiment, the inference method predicts the existence of cell-cell interactions, correctly mirroring the strong intercellular contacts that are present in the experiment. In the second experiment, dendritic cells migrate in a chemokine gradient. Our inference analysis does not provide evidence for interactions, indicating that cells migrate by sensing independently the chemokine source. According to this prediction, we speculate that mature dendritic cells disregard intercellular signals that could otherwise delay their arrival to lymph vessels.

Copyright © 2020
The Authors, some
rights reserved;
exclusive licensee
American Association
for the Advancement
of Science. No claim to
original U.S. Government
Works. Distributed
under a Creative
Commons Attribution
NonCommercial
License 4.0 (CC BY-NC).

$$\vec{s}_i = \frac{\vec{V}(i)}{V(i)} \quad \text{Normalized velocity}$$

The ME distribution consistent with the measures is

$$P(\{\vec{s}_i\}) = \frac{1}{Z(\{\vec{h}_i, J_{ij}\})} \exp \left[\frac{1}{2} \sum_{i=1}^N \sum_{j=1}^N J_{ij} \vec{s}_i \vec{s}_j + \sum_{i=1}^N \vec{h}_i \vec{s}_i \right]$$

MEA \rightarrow Most likely estimate for parameters $\{\mathbf{J}_{ij}\}$ accounts for pairwise interactions
 $\{\mathbf{h}_i\}$ accounts for bias

$$J_{ij}, \vec{h}_i \quad \text{s.t.} \quad \begin{cases} \langle \vec{s}_i \vec{s}_j \rangle_{\text{th}} = \langle \vec{s}_i \vec{s}_j \rangle_{\text{exp}} \\ \langle \vec{s}_i \rangle_{\text{th}} = \langle \vec{s}_i \rangle_{\text{exp}} \end{cases}$$

Boltzmann-Gibbs distribution at $K_B T = 1$ of the Heisenberg model whose Hamiltonian is

$$H(\{\vec{s}_i\} | \{J_{ij}, \vec{h}_i\}) = \frac{1}{2} \sum_{i=1}^N \sum_{j=1}^N J_{ij} \vec{s}_i \vec{s}_j - \sum_{i=1}^N \vec{h}_i \vec{s}_i$$

Langevin dynamics that allows the system to relax toward equilibrium

$$\frac{d\vec{s}_i}{dt} = -\frac{dH}{d\vec{s}_i} + \vec{\eta}_i(t) = \sum_{j=1}^N J_{ij} \vec{s}_j + \vec{h}_i + \vec{\eta}_i(t)$$

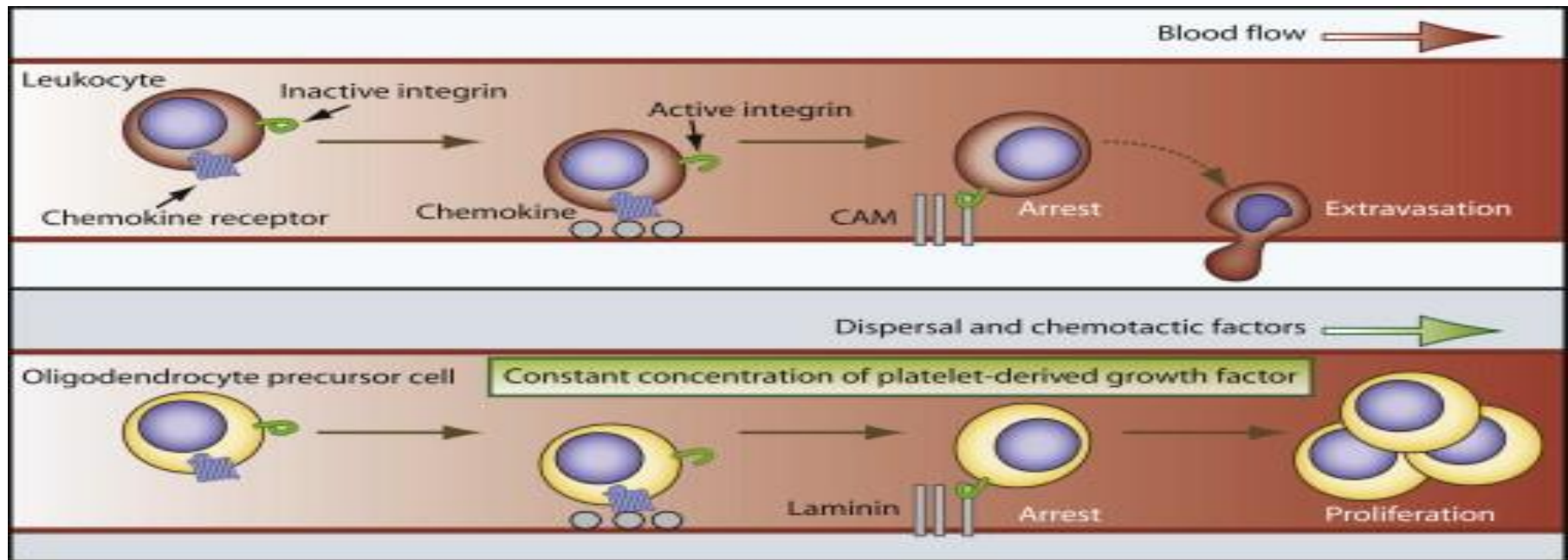
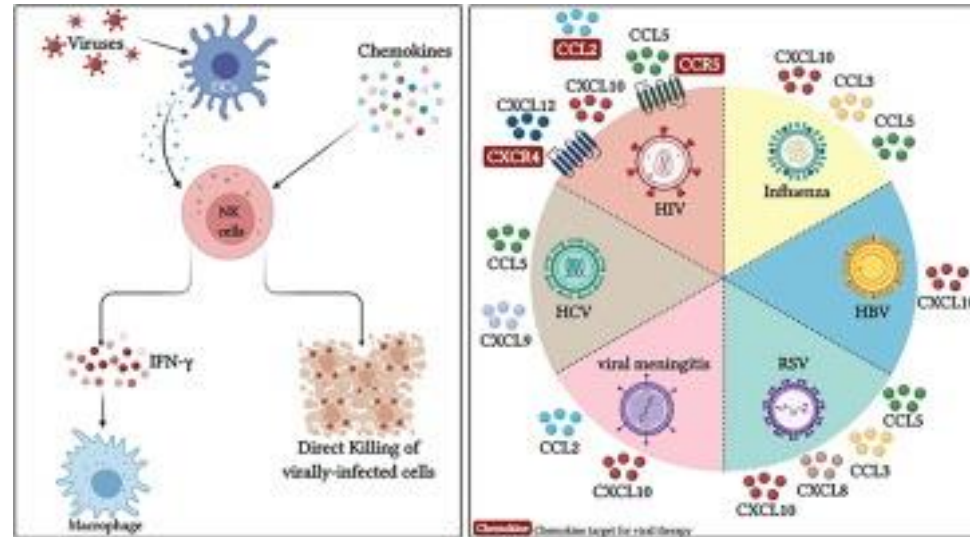
A big conceptual obstacle: at difference w.r.t. neural dialogues or flocks of birds, here leukocytes can not communicate «instantaneously» → **constraining the equal-time correlator is a huge mistake!**

NO!!!

$$\langle \vec{S}_i(t) \vec{S}_j(t) \rangle_{theor} = \langle \vec{S}_i(t) \vec{S}_j(t) \rangle_{exp}$$

$$\langle \vec{S}_i(t) \vec{S}_j(t + \tau) \rangle_{theor} = \langle \vec{S}_i(t) \vec{S}_j(t + \tau) \rangle_{exp}$$

YES!!!



Inverse modeling of time-delayed interactions via the dynamic-entropy formalism

$$\max_P S[P] \quad (7)$$

subject to

$$\int \mathcal{D}s P[s] M(s) = M^E, \quad (8)$$

$$\int \mathcal{D}s P[s] R(\tau, s) = R^E(\tau), \quad 1 \leq \tau \leq \tau_M, \quad (9)$$

$$\int \mathcal{D}s P[s] = 1. \quad (10)$$

To solve Eqs. (7) to (10), we introduce the Lagrangian multipliers $\mathbf{J} \equiv \{J_\tau\}_{\tau=1}^{\tau_M}$ and $\mathbf{H} \equiv \{H_\ell\}_{\ell=1}^D$, and obtain

$$P[s] = \frac{1}{Z} \exp \left[\sum_{t=\tau_M+1}^{N_T} \sum_{i=1}^N s_i^t \cdot \left(\frac{1}{N} \sum_{\tau=1}^{\tau_M} J_\tau \sum_{j=1}^N s_j^{t-\tau} + \mathbf{H} \right) \right], \quad (11)$$

Note: Markovian dynamics is not recovered!

Note: estimating tau gives to experimentalists Precious information (e.g. on the mass of the eventually unknown Signalling protein)...

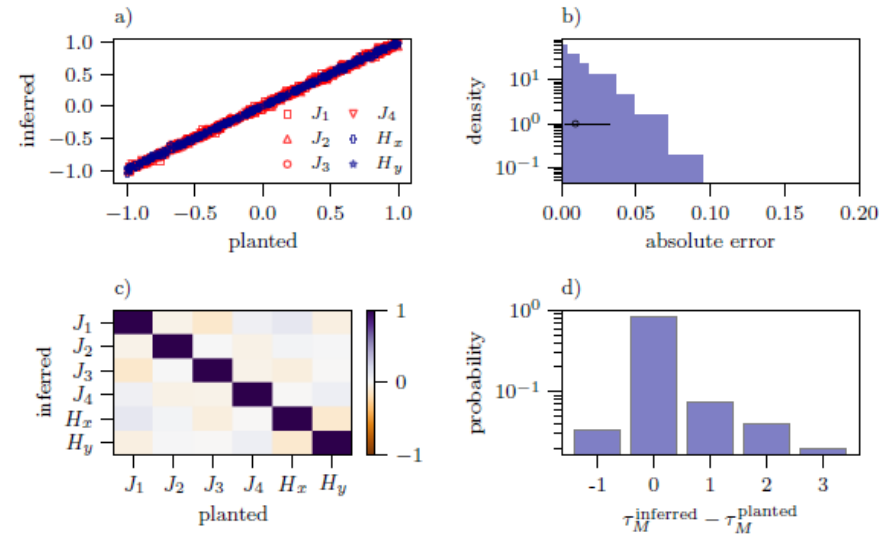
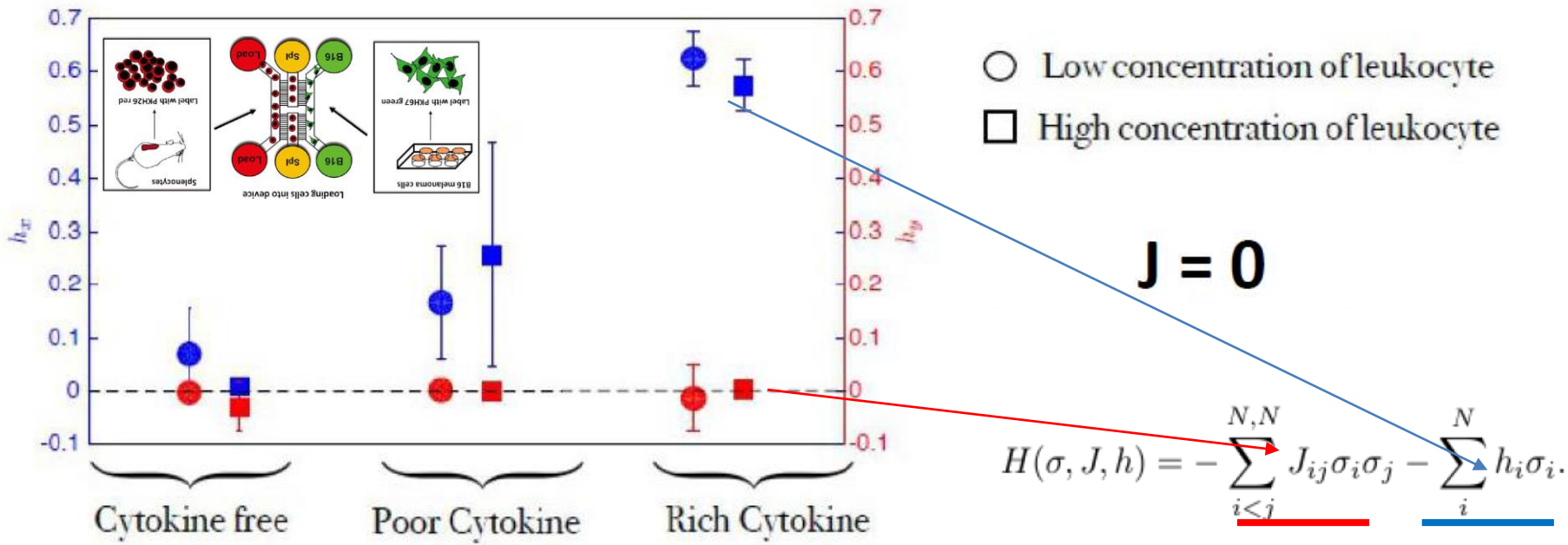
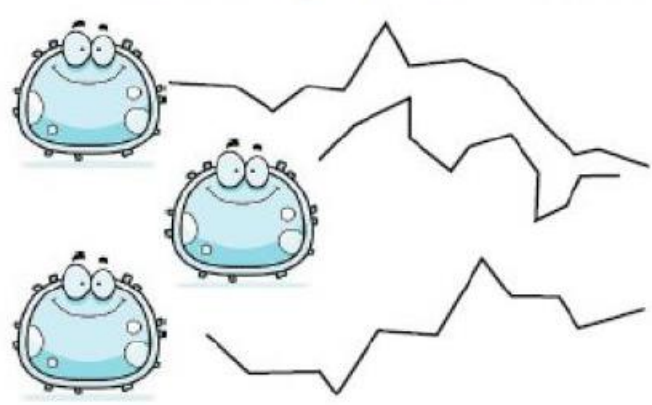


FIG. 1. Test of the statistical-inference method, where the Heisemberg-Kuramoto model is chosen as planted model. Here $D = 2$, $\tau_M = 4$, $\sigma = 0.1$, and we drew 150 planted parameters $J_1, \dots, J_{\tau_M}, H_x, H_y$ independently and identically from a uniform distribution over the range $(-1, 1)$. a) Scatter plot of planted vs inferred parameters: b) Histogram of the absolute error between \mathbf{J}, \mathbf{H} planted and \mathbf{J}, \mathbf{H} inferred: for each realisation of the process we calculate $|\mathbf{J}^{\text{inferred}} - \mathbf{J}^{\text{planted}}|$ and $|\mathbf{H}^{\text{inferred}} - \mathbf{H}^{\text{planted}}|$ and the related $150 \times (D + \tau_M)$ components make up the sample; the black dot represents the average and the black horizontal line represents a confidence interval of 68%; the average error is around $\sim 10^{-2}$, which is the expected amount of error given the size of the planted dataset. c) Pearson correlation matrix between planted and inferred parameters: as expected distinct kinds of parameters, e.g., \mathbf{H} and \mathbf{J} , are uncorrelated. d) Histogram of $\tau_M^{\text{inferred}} - \tau_M^{\text{planted}}$ obtained for the 150 realisations of the process.

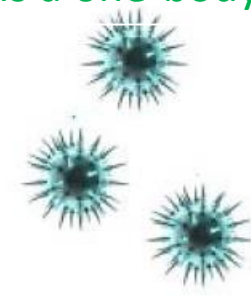
Results on chemoattractant gradient confirm no interactions during dendritic cell migration.
Note that the growth of the field (i.e. the gradient) is well captured (blue points)



Leukocytes in the presence of cytokines gradient display a drift which qualitatively affects motion
 No evidence of qualitative effects stemming from leukocyte interactions.

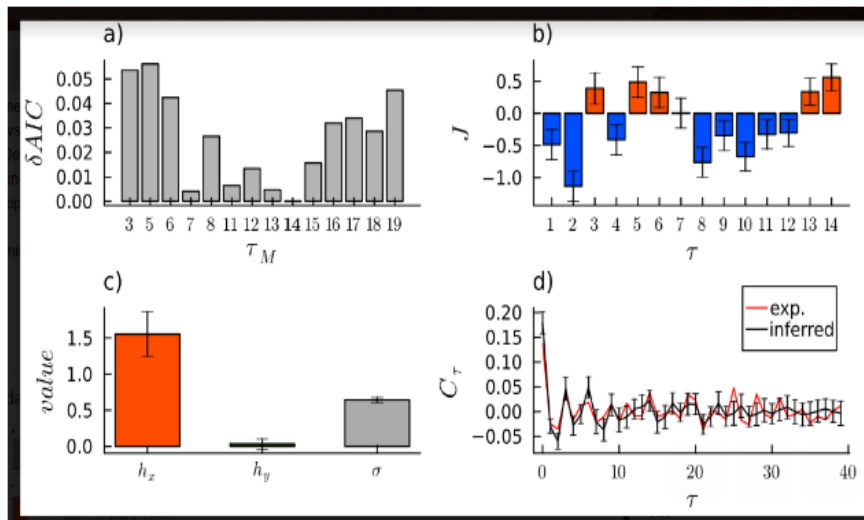
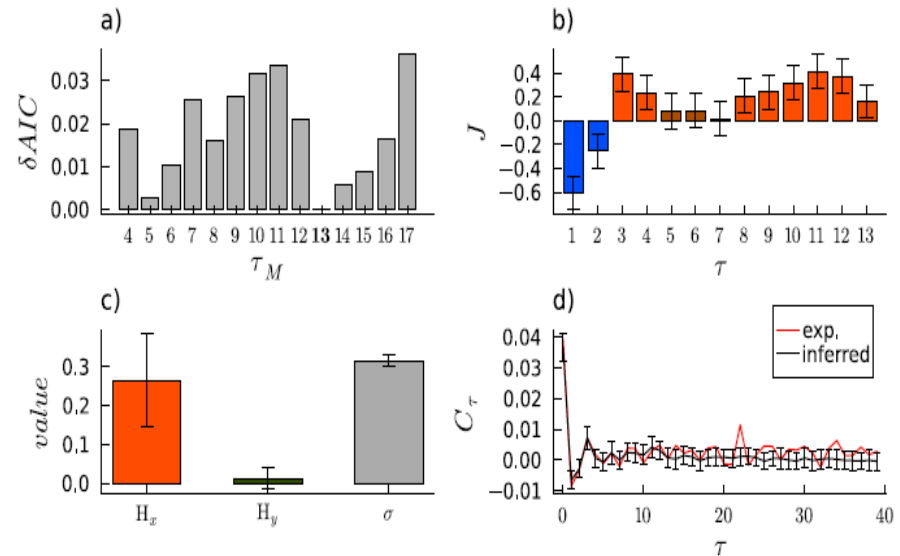
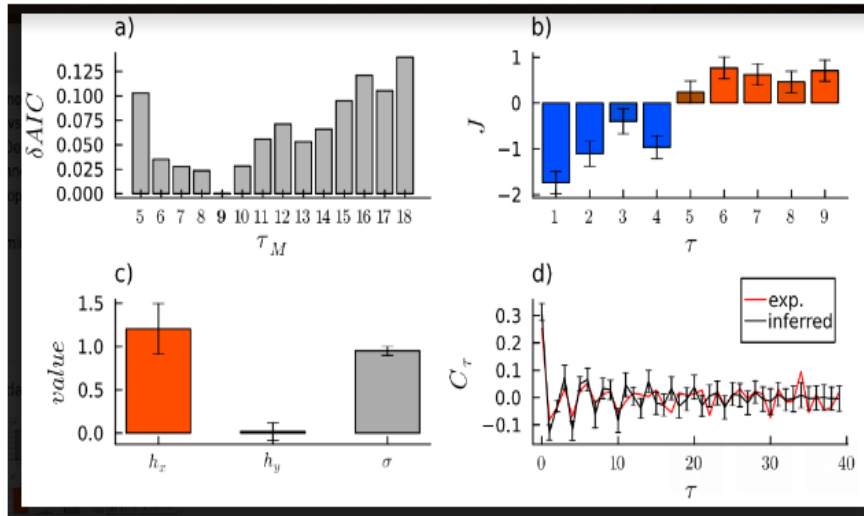


Dendritic migration to melanoma cancer is a one-body phenomenon!

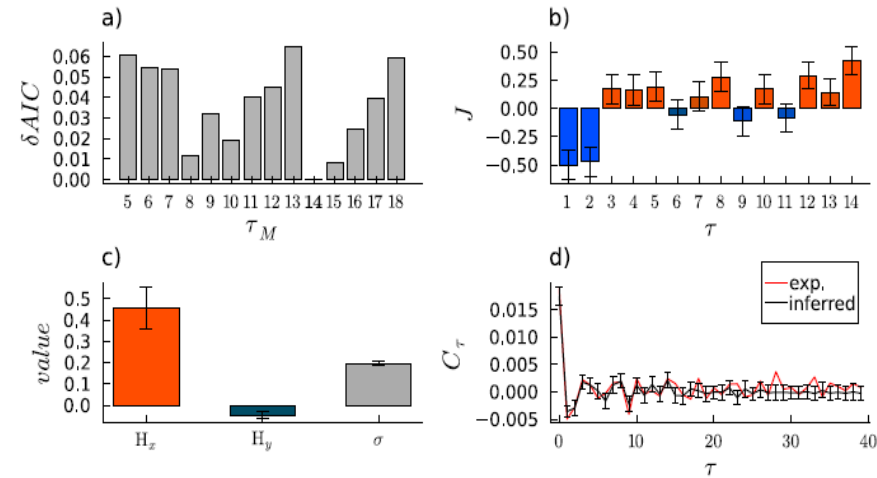


Real test cases: in upper plots different white cells undergo in a wound healing.

Dataset [A]



Dataset [B]



Real test cases: in lower plots different white cells undergo collective migration to antigen.

RESEARCH ARTICLE | BIOPHYSICS AND COMPUTATIONAL BIOLOGY

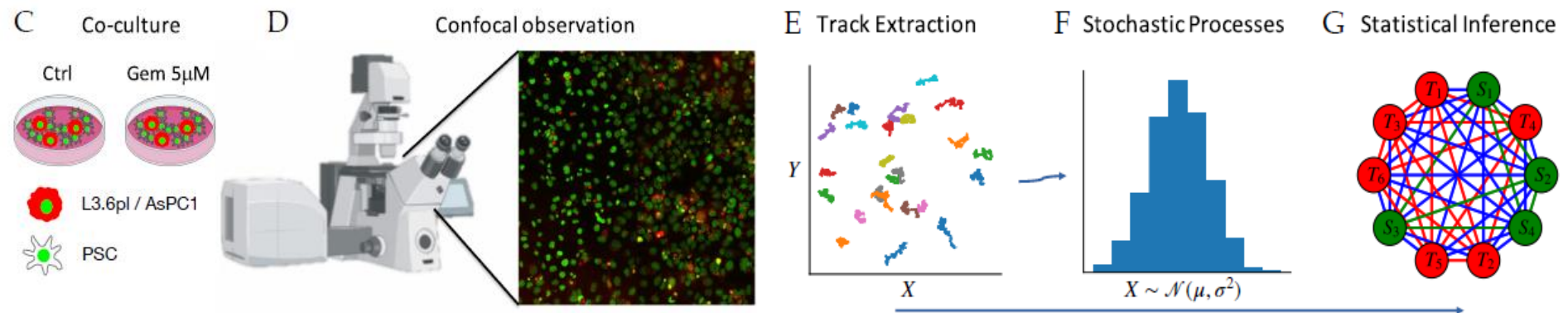


Quantifying heterogeneity to drug response in cancer–stroma kinetics

Francesco Alemanno , Marta Cavo, Donatella Delle Cave , , and Loretta L. del Mercato   [Authors Info & Affiliations](#)

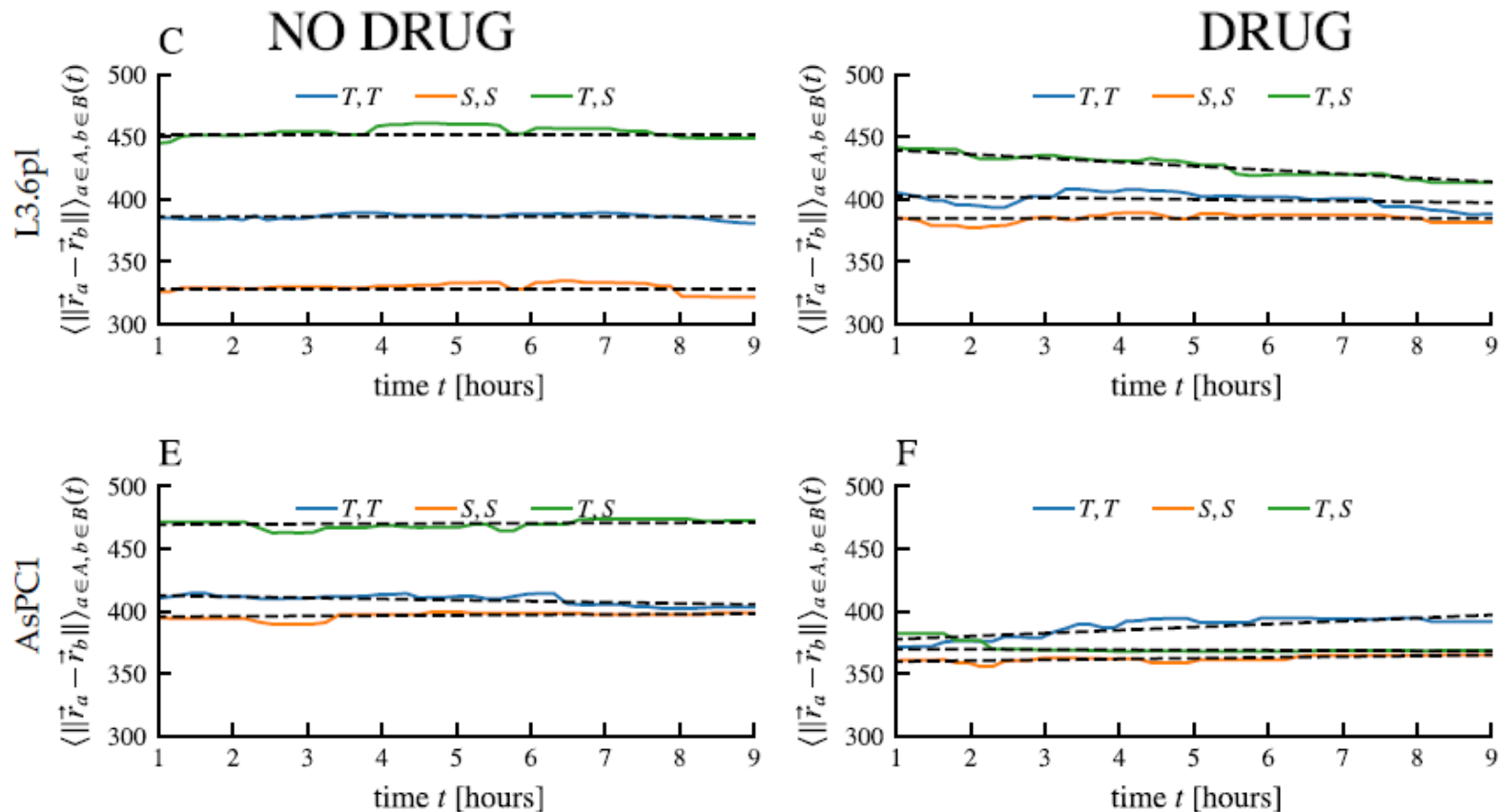
Edited by Michele Castellana, Institut Curie, Paris, France; received December 13, 2021; accepted February 4, 2023, by Editorial Board Member Mehran Kardar

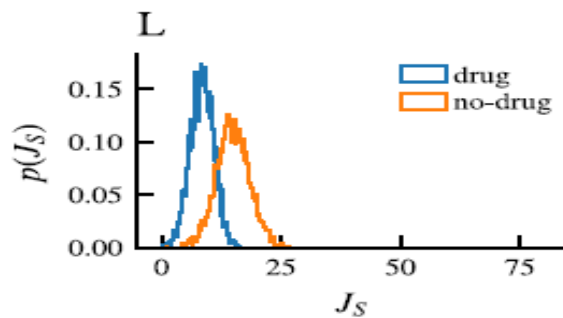
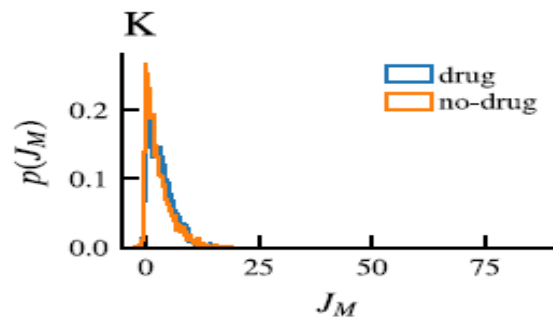
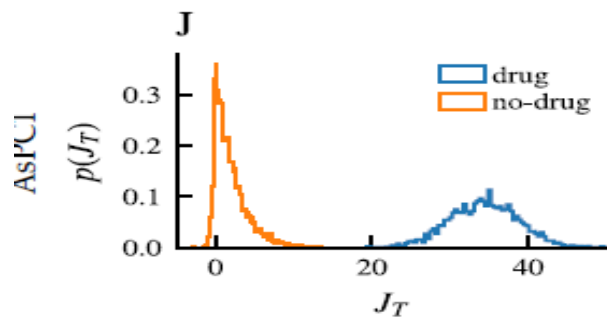
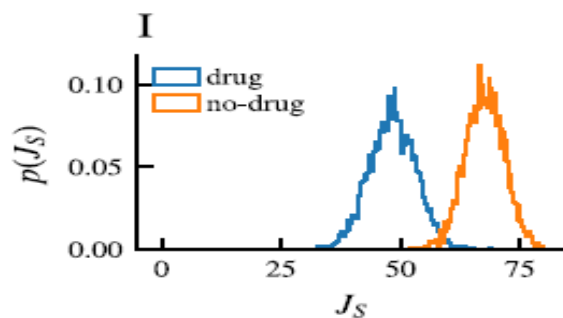
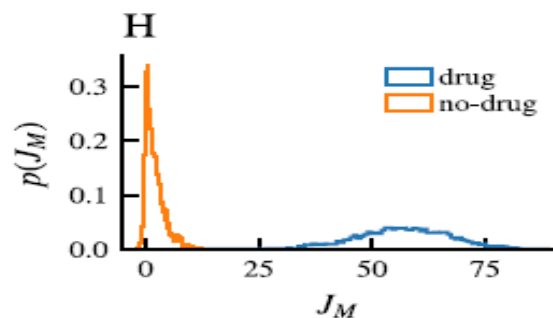
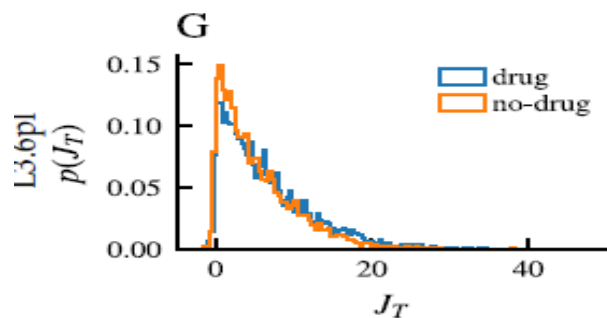
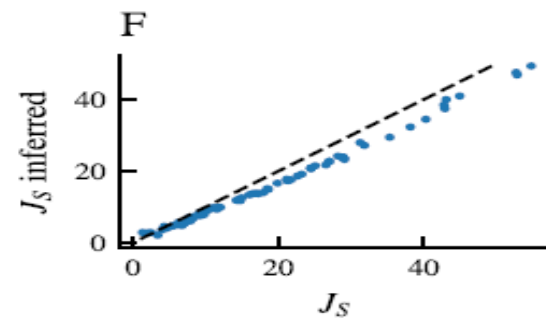
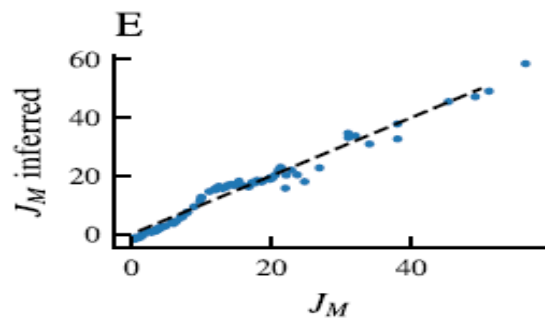
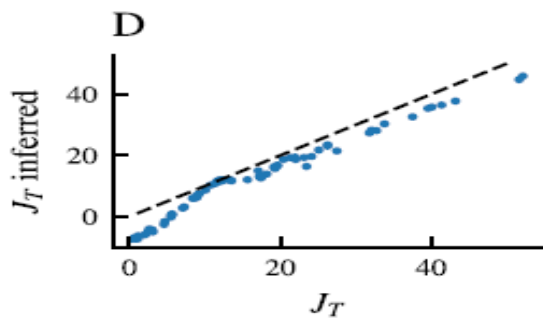
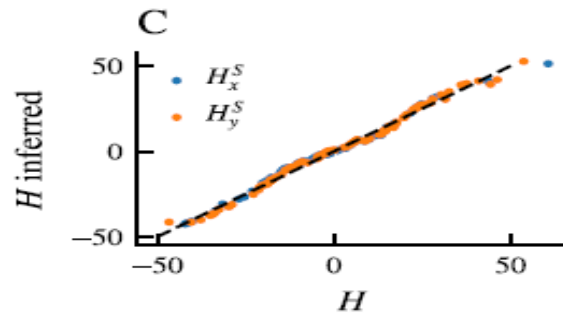
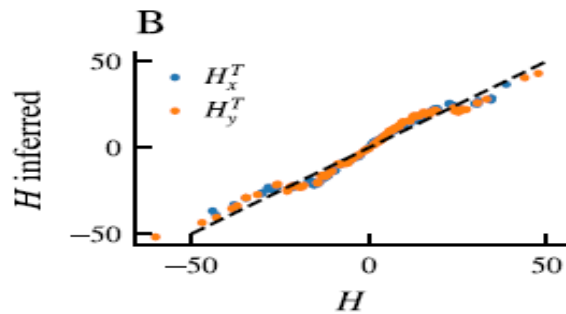
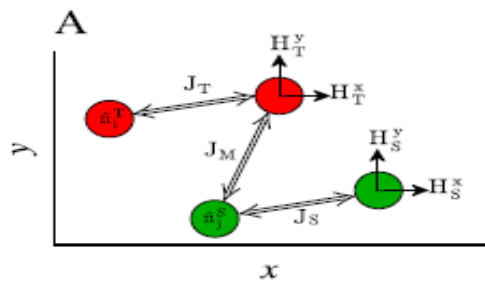
March 10, 2023 | 120 (11) e2122352120 | <https://doi.org/10.1073/pnas.2122352120>



What chemotherapy should I administer to the patient?

A major problem is that cancerous cells try to elude immunosurveillance...





Clinical outcomes are in agreement with math prediction (flow cytometer count of dead cells)

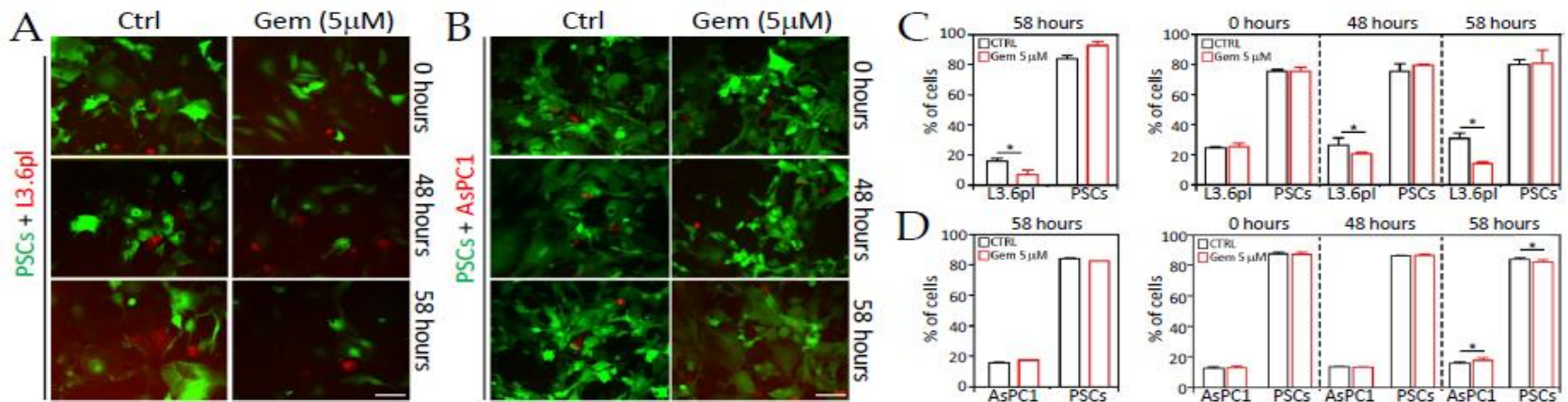


Fig. 4. Fluorescence imaging of tumor-stroma co-cultures during chemotherapy and evaluation of cell proliferation. Panel A) Representative fluorescence images of L3.6pl cells (red) co-cultured with PSCs (green), in the presence or absence of 5µM gemcitabine (Gem) for 0, 48 and 58 hours. Scale bars: 100µm. Panel B) Representative fluorescence images of AsPC1 cells (red) co-cultured with PSCs (green), in the presence or absence of 5µM Gem for 0, 48 and 58 hours. Scale bars: 100µm. Panel C) Percentage of L3.6pl and PSCs cells after treatment with 5µM Gem, counted with haemocytometer (left graph) or with flow cytometer (right graph) at the indicated times. $n \geq 3$. Panel D) Percentage of AsPC1 and PSCs cells after treatment with 5µM Gem, counted with haemocytometer (left graph) or with flowcytometer (right graph) at the indicated times. $n \geq 3$; $p \leq 0.05$.

...toward Precision & Personalized Medicine: works in fieri...

THANK YOU FOR YOUR GENTLE ATTENTION!!!

Ps) just in case: more on www.adrianobarra.com

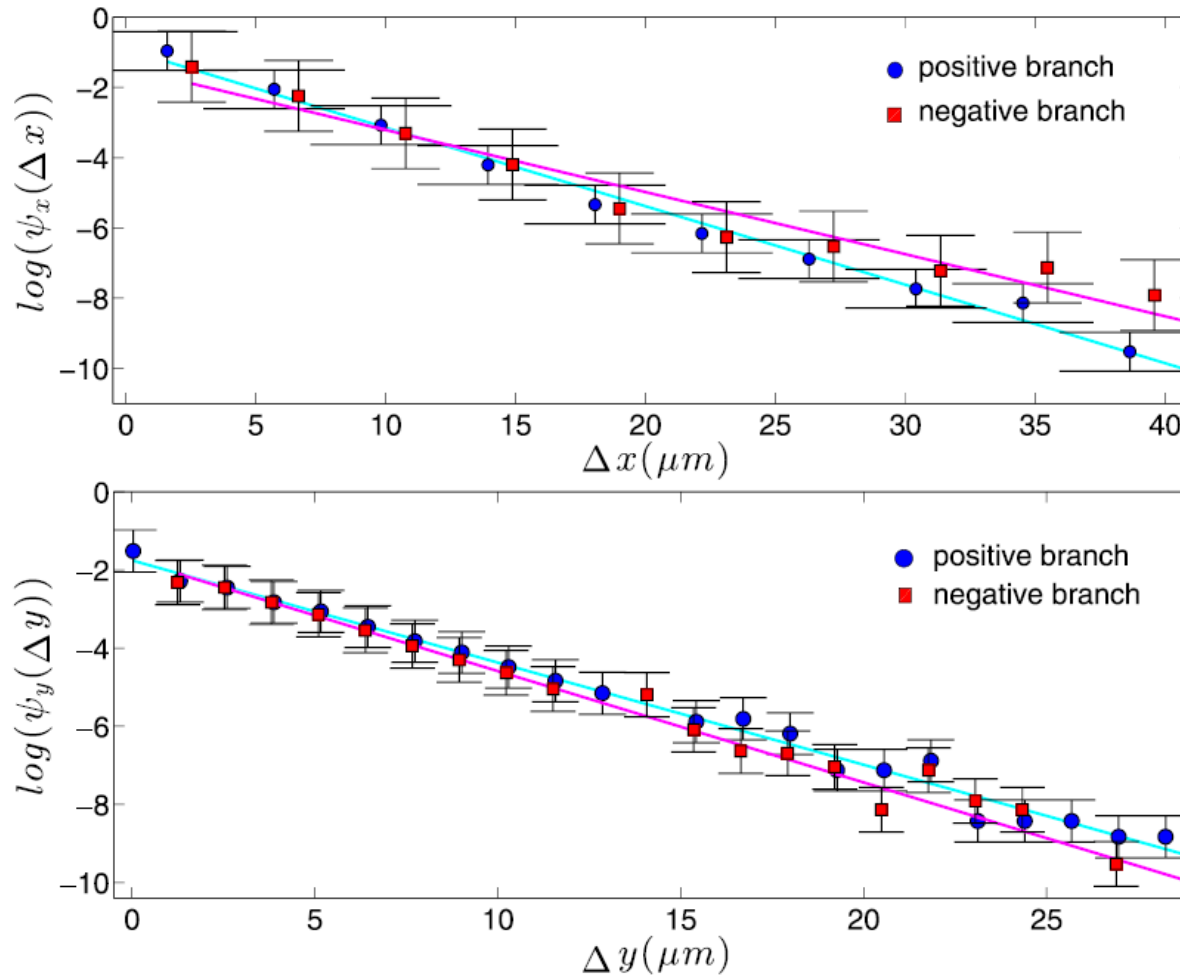


Figure 6 | Logarithm of the probability distribution for the step length along the x direction (upper panel) and along the y direction (lower panel). Experimental data (symbols) with standard errors are fitted by the exponential distribution (solid line) given by Eq. 8. All fits display $R^2 \approx 0.99$. The best fit coefficients are reported in Tab. I, where a comparison between average values from experiments and theoretical description is also provided.

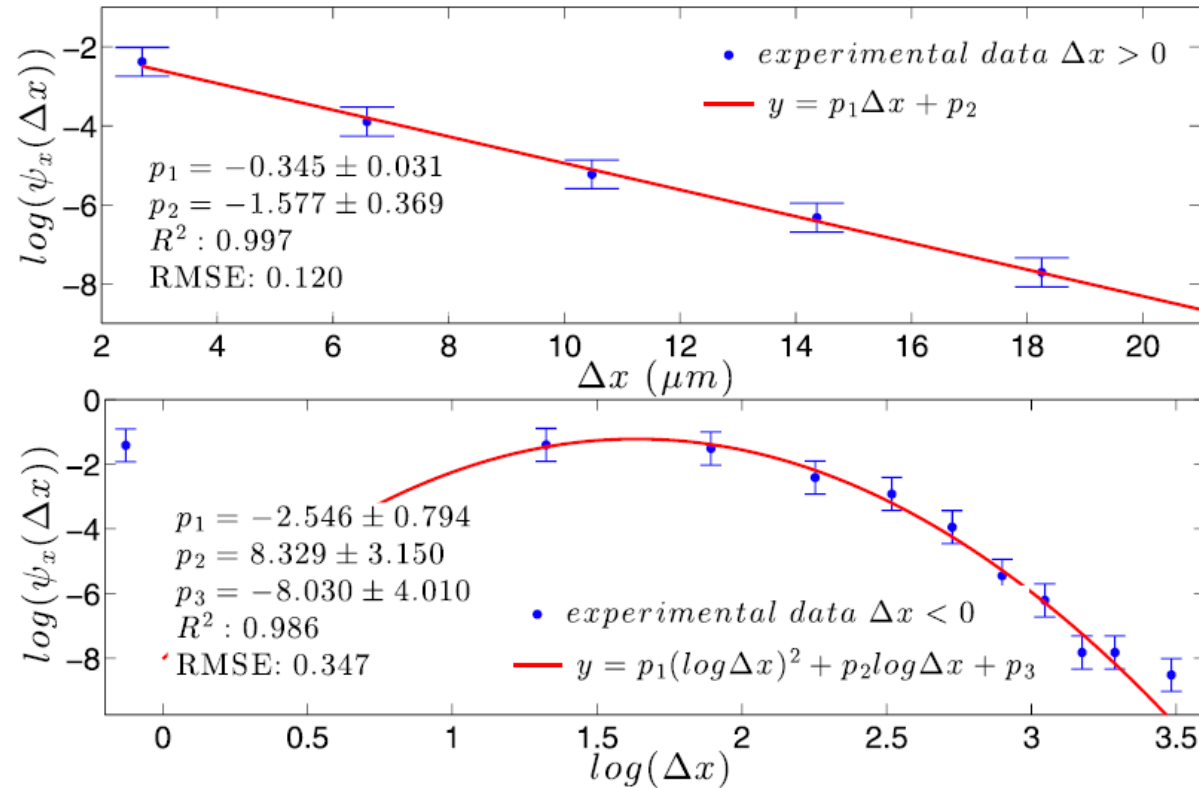


Figure 11 | $\psi_x(\Delta x)$ of WT-PRE splenocytes along the positive direction (upper panel, notice the semilogarithmic scale) and along the negative direction (lower panel, notice the logarithmic scale). Analogous plots are obtained for the y direction (not shown). Experimental data of the distributions (\bullet) with standard errors are compared with best fits (solid line). Note that the distribution is broadened along the negative x direction (and, analogously, along the positive y direction).




nature communications

Explore content \vee About the journal \vee Publish with us \vee

[nature](#) > [nature communications](#) > [articles](#) > article

Article | [Open Access](#) | Published: 05 July 2021

Cell migration guided by long-lived spatial memory

[Joseph d'Alessandro](#) , [Alex Barbier--Chebbah](#), [Victor Cellerin](#), [Olivier Benichou](#), [René Marc Mège](#), [Raphaël Voituriez](#)  & [Benoît Ladoux](#) 

nature communications

Explore content \vee About the journal \vee Publish with us \vee

[nature](#) > [nature communications](#) > [articles](#) > article

[Open Access](#) | Published: 25 June 2015

Cell migration and antigen capture are antagonistic processes coupled by myosin II in dendritic cells

[Mélanie Chabaud](#), [Mélina L. Heuzé](#), [Marine Bretou](#), [Pablo Vargas](#), [Paolo Maiuri](#), [Paola Solanes](#), [Mathieu Maurin](#), [Emmanuel Terriac](#), [Maël Le Berre](#), [Danielle Lankar](#), [Tristan Piolot](#), [Robert S. Adelstein](#), [Yingfan](#)